

Fermi National Accelerator Laboratory

FERMILAB-Conf-92/83

Energy Deposition and Radiation Shielding in the Pbar Source at Fermilab

C. Bhat

*Fermi National Accelerator Laboratory
P.O. Box 500, Batavia, Illinois 60510*

March 1992

Invited talk at the *International Workshop on Beam Induced Energy Deposition*, November 19-22, 1991, SSC Laboratory, Dallas, Texas.

Disclaimer

This report was prepared as an account of work sponsored by an agency of the United States Government. Neither the United States Government nor any agency thereof, nor any of their employees, makes any warranty, express or implied, or assumes any legal liability or responsibility for the accuracy, completeness, or usefulness of any information, apparatus, product, or process disclosed, or represents that its use would not infringe privately owned rights. Reference herein to any specific commercial product, process, or service by trade name, trademark, manufacturer, or otherwise, does not necessarily constitute or imply its endorsement, recommendation, or favoring by the United States Government or any agency thereof. The views and opinions of authors expressed herein do not necessarily state or reflect those of the United States Government or any agency thereof.

Energy Deposition and Radiation Shielding in the Pbar Source at Fermilab

C.M. Bhat

Fermi National Accelerator Laboratory

P.O. Box 500, Batavia, Illinois 60510*

January 1992

1 Introduction

Recently, because of the very high energy and very high luminosity accelerators being planned, built or upgraded, accurate evaluation of the total energy deposition and maximum energy density in the beam line elements are becoming more and more important issues. In an accelerator at lower beam intensities and/or lower radiation levels many of the beam line elements will behave nearly normal. But one might expect drastic changes in the material properties of these elements under high radiation environment and many times some of these elements might end up in catastrophic failures. For example, some of the failures of the Lithium lens and the 8GeV momentum analyzing magnet (called, pulsed magnet) in the antiproton production target station at Fermilab are believed to be related to the above types of problems. At present, measured data under controlled conditions on interaction of the particles with matter are only up to a maximum energy of 1TeV (Fermilab) and only a very few experiments are dedicated to investigate energy deposition and star densities. Also a consistent description of all the data with existing hadron interaction models is not fully satisfactory even at these energies. Therefore an extension of any of the existing models to SSC energy (i.e. 20TeV) to build beam line elements, might become questionable and the usage of the results of calculations should be done with enough safety margin. So it is desirable to understand the low energy data carefully. At SSC, the radiation levels under normal operating conditions or energy depositions under accidental losses of the beam can be much higher than any of the existing high energy accelerators. Hence the energy deposition related problems become key points in designing and determining life

Table I. Some luminosity upgrade parameters for antiproton source and Tevatron at Fermilab.

		Present(1989)	Upgrade
Antiproton Source	Proton Energy	120 GeV	120GeV
	Target	W, Ta, Cu	Cu (?)
	antiproton Energy	8GeV	8GeV
	proton/bunch	1.75×10^{12} (average)	5.0×10^{12} (average)
	Beam spot size	.08 - .012cm(average) (average $\sigma = 0.015$ cm)	.01cm(average)
	Spill time and δt	1.6 μ sec 2.6sec	1.6 μ sec and 1.5sec
	Stacking rate	2.0×10^{10} (Max.)	17.0×10^{10}
	Maximum Stack	120 mAmp	200.0mAmp
Antiproton Parameters in Tevatron	Antiproton/bunch	2.9×10^{10}	3.7×10^{10}
	Number of Bunches	6	36
	ϵ_{pbar}	18π	22π
	ϵ_{pbar}	18π	22π
	$\delta\nu$ / crossing	0.002	.008

time of the many beam line elements like magnets and kickers etc..

At Fermilab we have a number of upgrade plans related to luminosity increase. They are primarily a) installation of the proton and antiproton beam separators b) antiproton source improvement c) linac 200-400MeV upgrade and d) construction of Main injector. Table I summarizes some parameters for Fermilab upgrade¹. During 1989 collider run the maximum luminosity (L) reached was about $1.6 \times 10^{30} \text{ cm}^{-2} \text{ sec}^{-1}$. To increase L an improved performance of the antiproton source is very important. The antiproton beam parameters in the Tevatron² are also shown in the table I. For the future collider runs the expected intensity of the proton beam on the antiproton target will be increased by about three times and the beam spot size (σ) will be decreased by about 1.5 times. Due to these improvements, the antiproton yield will be increased by a factor of more than three. But, at the same time, the total energy and the star densities (number of interactions/gm or cc) deposited in various beamline elements will also go up and might affect their performance. Hence, a good understanding of the failures of the beamline elements during previous collider runs has become extremely important to see whether these are related to beam-induced energy deposition. This needs a realistic evaluation of the energy and star densities in all the elements and careful measurements of the same. Apart from these, radiation shielding should also be re-evaluated and necessary steps should be taken from the point of view of environmental safety and health.

2 Antiproton Source Beamline Elements and Energy Deposition

From energy deposition point of view, the beamline elements in the antiproton source can be broadly classified into two categories based on beam energy and intensity of the beam: 1) beam line elements in the target hall and 2) elements downstream of the target hall (like AP2, AP3 beam lines, Debuncher and Accumulator rings). The yield of the 8GeV antiproton is about 5.0×10^{-5} /proton (for $\sigma = .015\text{cm}$) at 120 GeV. A very small fraction of the secondary beam will enter into the AP2 beam line through the downstream pulsed dipole magnet tuned to select negatively charged 8GeV particles. The radiation level down stream of the pulsed magnet is several orders of mag-

nitude smaller than that seen near the antiproton production target. Hence, not much emphasis is given here to the beam line elements down-stream of the analyzing magnet except for radiation shielding considerations. The beam line elements in the target station are antiproton target, lithium lens, pulsed magnet and 120GeV beam dump. The beam dump was originally built to receive 3.0×10^{12} proton/pulse at 150GeV with enough safety margin. Presently the beam energy is about 25% lower than the original design value. Hence, we can go up in the incident proton beam intensity by the same amount. (The planned incident proton beam intensity for the upgrade of 5×10^{12} p/pulse should be still within the safety limit). At present no further upgrade of the 120GeV beam dump is undertaken. But in future this issue should also have to be addressed.

An evaluation of the energy deposition and star densities have been made by using Monte Carlo codes MARS10³ and wherever possible we compared the results with the calculations done using either CASIM⁴ and/or FLUKA⁵.

2.1 Target

Figure 1a shows an antiproton production target module similar to the one used during 1987 and 1989 collider runs. This has four different target materials viz, copper, tantalum, aluminium and heavy metal. Each of them has been sandwiched between two brass cooling disks. The target is cooled by using forced air. Before installing, the target will be completely covered with a titanium (high melting point and low density material) cylindrical jacket (shown in the figure 1a by the side of the target module). The target in the vault will be having four degrees of freedom viz., motion along x, y, z-axis and rotation about its symmetric axis.

Figure 1b and 1c show an example of beam-induced effect on a heavy metal target. In this case, target was exposed to proton beam for a period of six months during the commissioning run in 1987. After cooling for two years a destructive analysis⁶ of the target has been carried out using the facility at Argonne National Lab. Clear indications have been seen about the void formation and etching of the target by the beam. Also fusing of the target with the cooling disks near the junctions and a number of cracks along surface of the target have been seen. Probably, shock waves are produced due to sudden increase in the local energy density within $1.6 \mu\text{sec}$ during the interaction of the beam with the target. These waves propagate through the

material and are reflected back from the relatively flat edges or interfaces. Destructive interference of these waves cause density depletion in certain region of the target and also cracks, resulting in permanent destruction of the target. This sort of shockwave induced processes are very much dependent upon the thermoelastic properties of the target material. The heavy metal being not a very good conductor of heat, during the beam interaction the temperature also might have gone up to a very high value. Thus the material melted and fused with the cooling disks.

In general, the target-damage mechanisms can be classified to fall in to two categories: a) long-term effects and b) single- pulse mechanisms. Long-term effects include the depletion of the target density, swelling of the target, void formation and target deterioration etc. These would mainly depend on how long the target is exposed to the beam. The single- pulse mechanism is dependent upon the beam spot-size and number of particles per pulse. Here the shock wave propagation and its intensity play very important role. Both these effects are dependent upon thermoelastic properties of the target material. During the 1987 collider run, the beam size and the intensity were of the order of .08cm and 1×10^{12} proton/pulse respectively. Also the target we have studied was in the beam for more than five months. We have observed both these phenomena. However, based upon our measurements it is difficult to say at which stage of beam bombardment one mechanism dominated over the other.

Thus from these studies we realized that the target has to be redesigned and further investigation should be made to select better target material in order to avoid possible structural damages to the target. This needs an accurate evaluation of energy density (ϵ), as a function of material properties, target geometry and the beam parameters. Figure 2 shows results of Monte Carlo calculations for the maximum energy density ϵ_{Max} in copper as a function of r.m.s. beam size σ . Here, we assume a symmetric gaussian distribution for the incident proton beam. Using this curve we have estimated that under normal operation during 1989 collider run, a maximum of about 785Joule/gm/pulse in the target has been reached. A comparison of this value with the melting point energy of copper ($E_{melt} = 668$ Joule/gm) suggests that certain regions of the target along the beam path might have reached melting point (assuming the heat loss due to thermal conduction is negligible during the beam spill time of $1.6\mu\text{sec}$). At beam intensities higher by a factor of three and σ smaller than 0.015cm, it is probable that there

will be noticeable amount of melting of the target even due to interaction of a single pulse. Figures 3a, 3b and 3c show energy densities as a function of z and r. Using these results we estimate total energy deposited in the target module as 264watts which is only 1.6% of the total beam energy.

The energy deposition calculated from a Monte Carlo code can be used to determine the instantaneous pressure developed in the target material during the beam spill time. For this we use Mie-Gruneisen equation of state. Figure 4 shows results of such calculations on some of the target materials of interest. We find that for the same amount of energy deposition the pressure developed will be about 4-5 times larger in iridium than in copper. We have looked into many materials⁷ and have concluded that copper is the best material from the point of view of thermoelastic properties. One can also think of a material made by suspending powder of high atomic weight and low density metal (like yttrium or zirconium) in copper so that the average atomic weight can be increased. (It is important to note that this type of material is not an alloy of copper because the thermal conductivity and elastic properties are mainly of copper.) In these targets pbar yield can also be increased by more than 10% as compared to pure copper target.

Based on above studies two methods have been suggested to upgrade the target. The first one is sweeping⁷ the primary 120GeV proton beam on the target in a circular fashion so that the energy is distributed in a larger volume within the beam-spill time. The difficulty in this method is designing down-stream radiation resistant kickers. Second one is to go for a new design for the target. Figure 5 shows⁸ one of the target modules proposed for study during the future collider run. In this design the emphasis are on efficient way of cooling the target and shock wave absorption. The present target module has four layers of holes with total of about 80 holes for cooling. Calculations showed that the first sets of holes surrounding the targetting region of .5in dia alone is good enough to reduce the shock waves intensity up to about 50%. Bench test of the target is very much encouraging. Study of the target with high intensity beam is planned and effort is being made to sort out single pulse mechanism and long term effects on the target material.

2.2 Li Lens and Pulsed Magnet

The lithium lens was originally designed⁹ for beam intensity of 2.5×10^{12} proton/pulse with beam spot size $\sigma = \sigma_x = \sigma_y = 0.0378$ cm. Figure 6

Table II. Energy Deposition in Li Lens.

Assembly	Device Name	ϵ GeV/p/gm	Joule/1E12 proton/pulse	Joule/5E12 proton/pulse
Li Lens	Be Window Assembly	0.0317	5.1	25.4
	Li Core	0.0811	13.0	65.0
	Ti Septum	0.82	131.0	657.0
	Steel Lens body	4.014	643.0	3215.0
Transformer	Inner Al Housing Assembly	.2742	44.0	220
	Inner Cu Conductor Bar	0.66	106.0	529.0
	Reminder Al Housing	0.1205	19.3	96.5
	Fe Core	.838	134.0	671.0
	Outer Cu Conductor Bar	.0694	11.0	56.0
	Upstream Primary plates	0.159	25.0	127.0
	Downstream Primary plates	0.1431	23.0	115.0
	Total		7.2	1155.2 (577 Watt)

Table III. A comparison of measured and calculated energy deposition for 120GeV protons at $1.7E+12p/pulse$.

		Li-lens	Pulsed Magnet
A	Joule Heating	3318Watt	230Watt
B	Heat taken away by water cooling	4133Watt	0.0
C	Radiation Loss	60Watt (Emissivity=.2)	1210Watt (Emissivity=.95, painted surface)
	Beam Induced Energy Deposition – B+C-A		
	Measured	875 watt	980 watt
	Calculated	981 watt	2000 watt

shows a schematic diagram of the present lens with its transformer. Table II displays the results of calculations on the energy deposition on various sections of the lens. We estimate total energy deposition in the lens to be about 2888watt for 5.0×10^{12} proton/pulse incident. The total energy deposition measured during the 1989 collider run agree with the calculation to within about 13%. (We expect the measured values of energy deposition

might have 30-40% errors mainly arising from convection losses which we could not estimate in our measurements.)

The pulsed magnet was standard 200-turn one meter long dipole magnet. It has an aperture of $1.77\text{cm} \times 1.77\text{cm}$. The distance between the lithium lens and the pulsed magnet is 69.95cm in the vault. Monte Carlo calculations estimate the energy deposition by a factor of two larger than the measured value. This difference may be associated with convection loss due to additional cooling of the modules by air blown in the vault which is difficult to estimate and not included in table-III. However, observations gave us a fairly good verification of the calculations of energy deposition.

As a result of above studies steps have been undertaken to improve the design in Li-lens as well as the pulsed magnet. Additional cooling lines have been implemented on the body of the lens. Our calculations show that this will enable us in keeping the lens cooler by about 20-25%. From the table II it is clear that a significant energy deposition takes place in the steel of the lens body. To cool this part of the lens more efficiently, a new design has to be implemented. For the pulsed magnet single turn water cooled magnet is designed and this module is ready to go into the vault.

3 Radiation Shielding for Antiproton Source

An evaluation of the adequacy of the radiation shielding in the antiproton source was made¹⁰ during the summer of 1991 in preparation for the future collider runs. We will briefly discuss here the criteria and the method adopted in the evaluation.

To calculate the residual gamma ray activity induced by a pulsed primary high energy beam incident on a target a realistic model¹¹ has been developed. This model uses the star densities predicted from Monte Carlo calculations to estimate the radiation level. The model has been used to predict the activation of one of the earlier Fermilab antiproton production targets. Properties of about 42 radioactive nuclei formed in the target whose life times are greater than five minutes have been considered. We find that the activation has been predicted quite well within 20%. To estimate the instantaneous dose rate one has to include properties of short lived radioactive nuclei in the interaction of high energy particles with the target material. This evaluation is relatively less accurate mainly because available information on the short lived radio

isotopes has large errors or are empirically deduced. Therefore one uses a constant conversion factor derived from measured values of activation and comparison with calculated star densities. For example one uses a conversion factor of $10.8 \mu\text{rem}(\text{star}/\text{cm}^3)$ for CASIM calculation. This conversion factor is cited in the Fermilab Radiation Guide¹² as appropriate for soil.

At Fermilab the maximum allowable radiation dose equivalent is set at $2500\text{mrem}/\text{year}$ ¹². Depending upon the beam intensity, beam energy and the material of the beam line elements the shielding criteria change. A summary of such shielding criteria are shown in table IV.

We have investigated the radiation pattern from a point loss in the pbar source enclosure due to the interaction of the beam with a magnet or other beamline elements. Here the calculations have been performed using CASIM. The

Table IV. Radiation shielding criteria.

		D(mr/hr)
1	No occupancy limit	1.0
2	Minimal occupancy	10.0
3	Signs and ropes	100.0
4	Signs, fences, locked gates	500.0
5	Signs, fences, interlocked gates	1000.0
6	Minimal occupancy 'non-accidents'	2.5
7	Signs and ropes 'non-accidents'	10.0

beam line enclosures in the antiproton source are almost flat and hence computer modelling in CASIM is fairly straight forward. Radiation measurements have also been conducted¹⁰ both during stacking as well as conditions similar to antiproton source study period. The measurements have been performed using sixty four radiation detectors. All of them were set for quality factor of five to give a reasonable estimate of the biological damage from neutrons but they over-estimate the hazards for gamma and beta radiations. All the data have been normalized to $3E12$ protons/pulse/2sec. A number of film badges have also been placed in the test area. The total dose from these were too small to establish the shielding criteria. The results of these measurements have been summarized in the table V. Using the criteria from table IV, the existing shieldings throughout the antiproton facility is re-evaluated. More measurements have been made after radiation shieldings have been added(Ref. 10) To cite some examples the radiation dose rate on the roof AP0 building was reduced to be 5-11mrem/hr, in the vault area it was a maximum of 300mrem/hr and near the closed loop water cooling system the maximum dose rate was 125mrem/hr. Thus our measurements showed the necessary shielding criteria have been achieved.

4 Summary

Beam-induced energy deposition and radiation damage of the pbar target, Li-lens and pulsed magnet mandate an upgrade of these systems. A new target has been designed and will be tested during future collider runs. In the upgrade of Li lens, new cooling systems have been added. This is designed to take away as much as 25% of the heat developed by the beam. The old pulsed magnet is being replaced by single-turn water cooled pulsed magnet. Radiation shielding studies and assessment and upgrade of the shielding have been done for the upgrade of the pbar source.

Author would like to thank J. Marriner, M. Gormley and K. Anderson for useful discussions.

Table V. Radiation measurements at AP0. Radiation dosage normalized to 3E12p/p 1800pph.

Radiation Source	Detector location	Target Condition	Radiation level before shielding
M:VT101	-Just outside the enclosure gate	Target in	950mr/h
	-Just inside the enclosure gate	Target in	4000mr/h
PQ6	berm above M:vt102	Target in	33mr/h
	-Directly above the hatch	Target in	4.6mr/h
Taret	directly above the berm	Target in	150mr/h
	-Work area outside the shielding wall	Target in	less than 10mr/h
	-On the top the shielding wall	Target in	720mr/h
	on the top vault	Target in	6300mr/h
	-On the roof	Target in	320-485mr/h
	-Penetration to the dump inside the locked gate	Target in	590mr/h
	-Penetration to the dump inside the locked gate	Target out	720mr/hr and a factor of five smaller at all other places

REFERENCES

* Operated by Universities Research Association Inc. under contract with the U.S. Department of Energy.

1. S.D.Holmes, Fermilab Conf. Rept. 91/141 (1991)
2. 'Design report Tevatron 1 Project (1984)'
3. N.V. Mokhov, MARS10 Manual, Fermilab, FN-509 (1989).
4. A. Van Ginneken, CASIM, Fermilab FN-272 (1975).
5. P.A. Aarnio et al, FLUKA86 user's guide TIS-RP/168 (1986).
6. M.Gormley, Fermilab private communications (1988).
7. C.M. Bhat and N.V.Mokhov, Fermilab, TM1585 (1989), C.M. Bhat, Pbar Note 485 (1989) and C.M. Bhat, Fermilab, TM1743 (1991).
8. K. Anderson, C.M. Bhat, J. Marriner and Z.Tang, An antiproton target design for increased beam intensity, Proc. of IEEE particle accelerator conference, 1991 San Francisco, CA, (1991) 1946.
9. A.J. Lennox, Energy deposition in the Li lenses, pbar note 204 (1982).
10. C. Bhat et al, 'Antiproton Source Shielding Report' Accelerator Division Internal Rept. (Sept. 1991).
11. C.M.Bhat and J.Marriner, Gamma ray activation of the Fermilab pbar target, Proc. of IEEE particle accelerator conference, 1991 San Francisco, CA, (1991)p 831.
12. L. Coulson et al, 'Radiation Guide Fermilab Fifth Edition 1988.

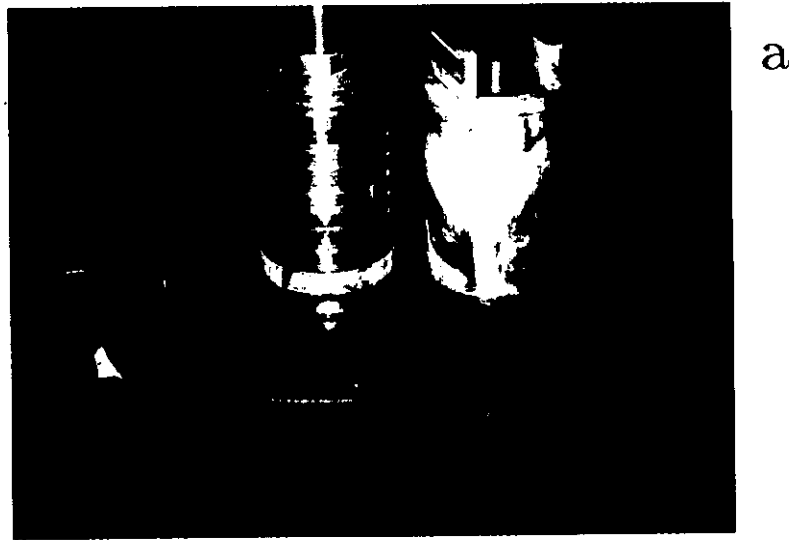


FIG. 1. An antiproton production target module similar to one used during 1987 and 1989 collider runs a) target (and a titanium jacket) before the beam interaction b) and c) effect of the 120GeV beam on the heavy metal target.

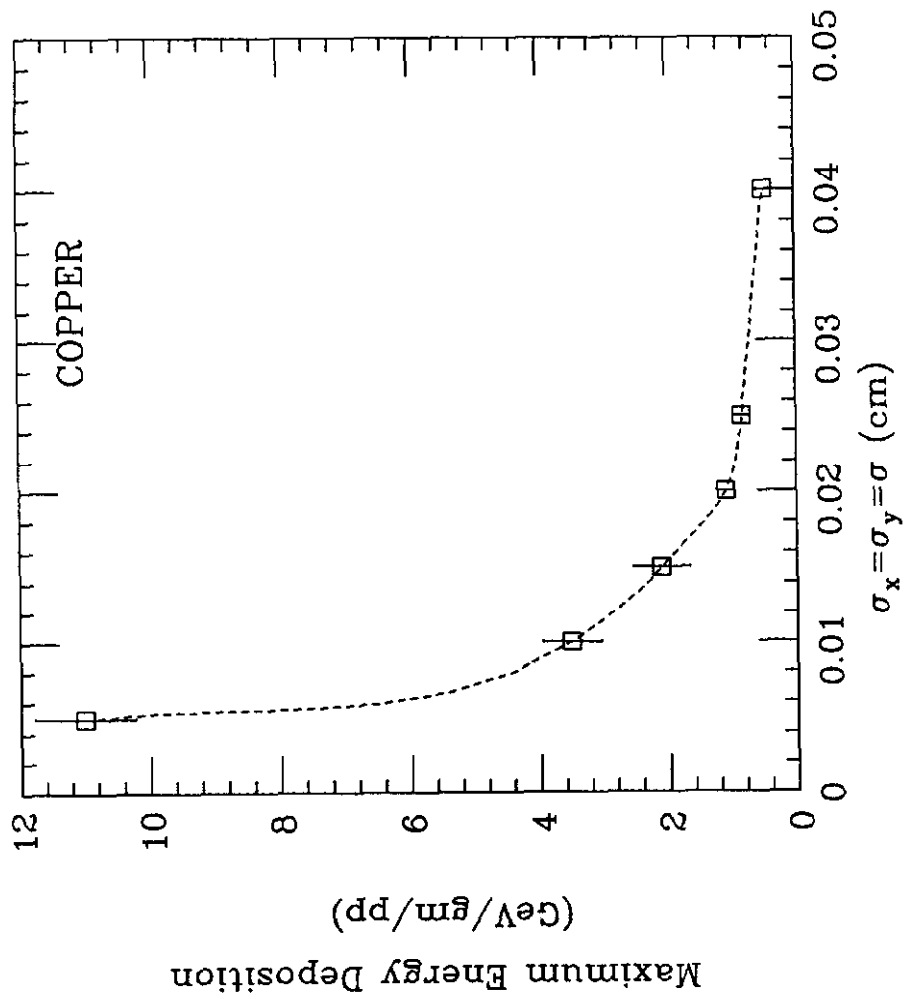


FIG. 2. Maximum energy deposition density in a copper target as a function of beam spot size.

COPPER

MARS10

120GeV/c

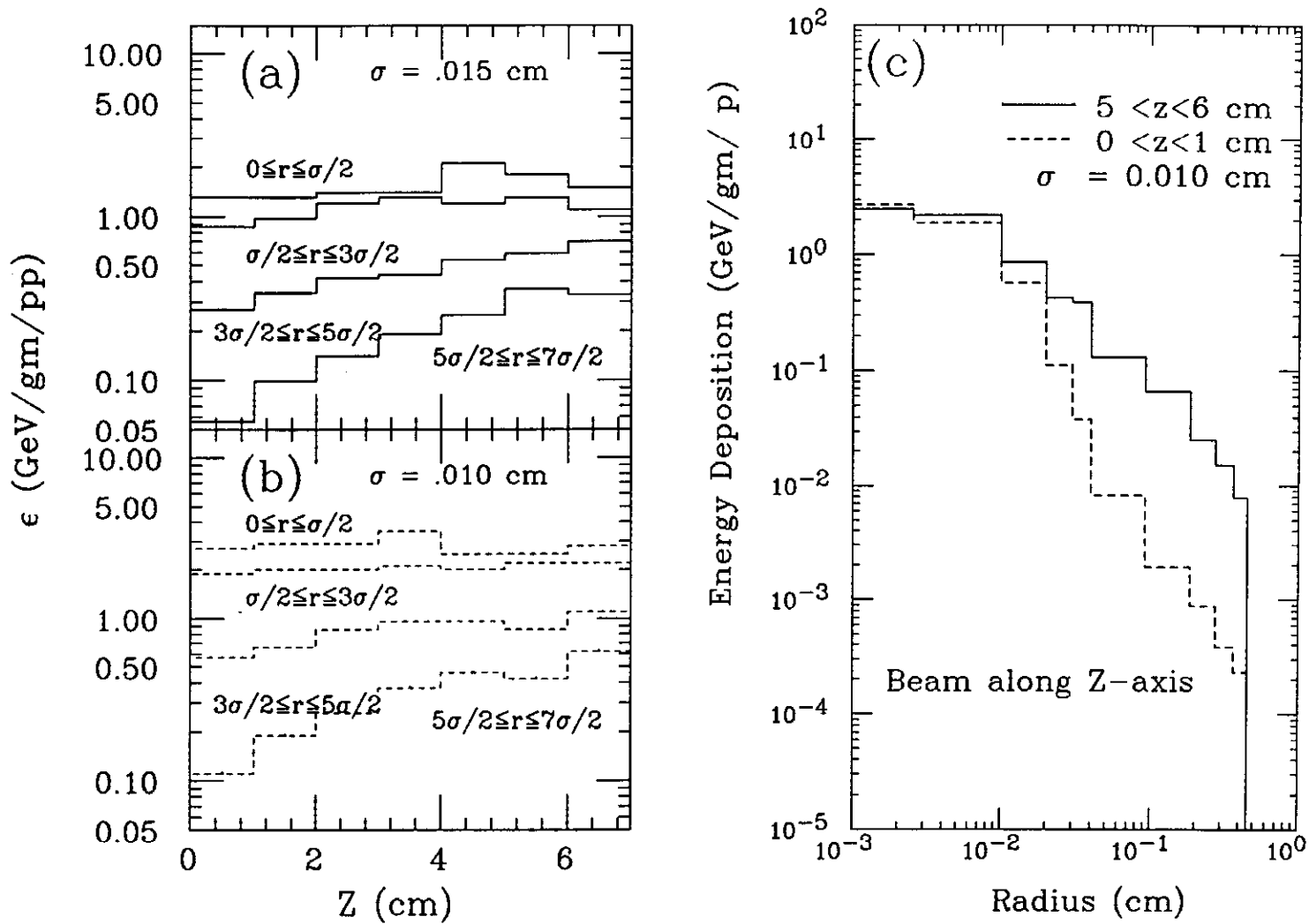


FIG. 3. Energy density as a function of r and z.

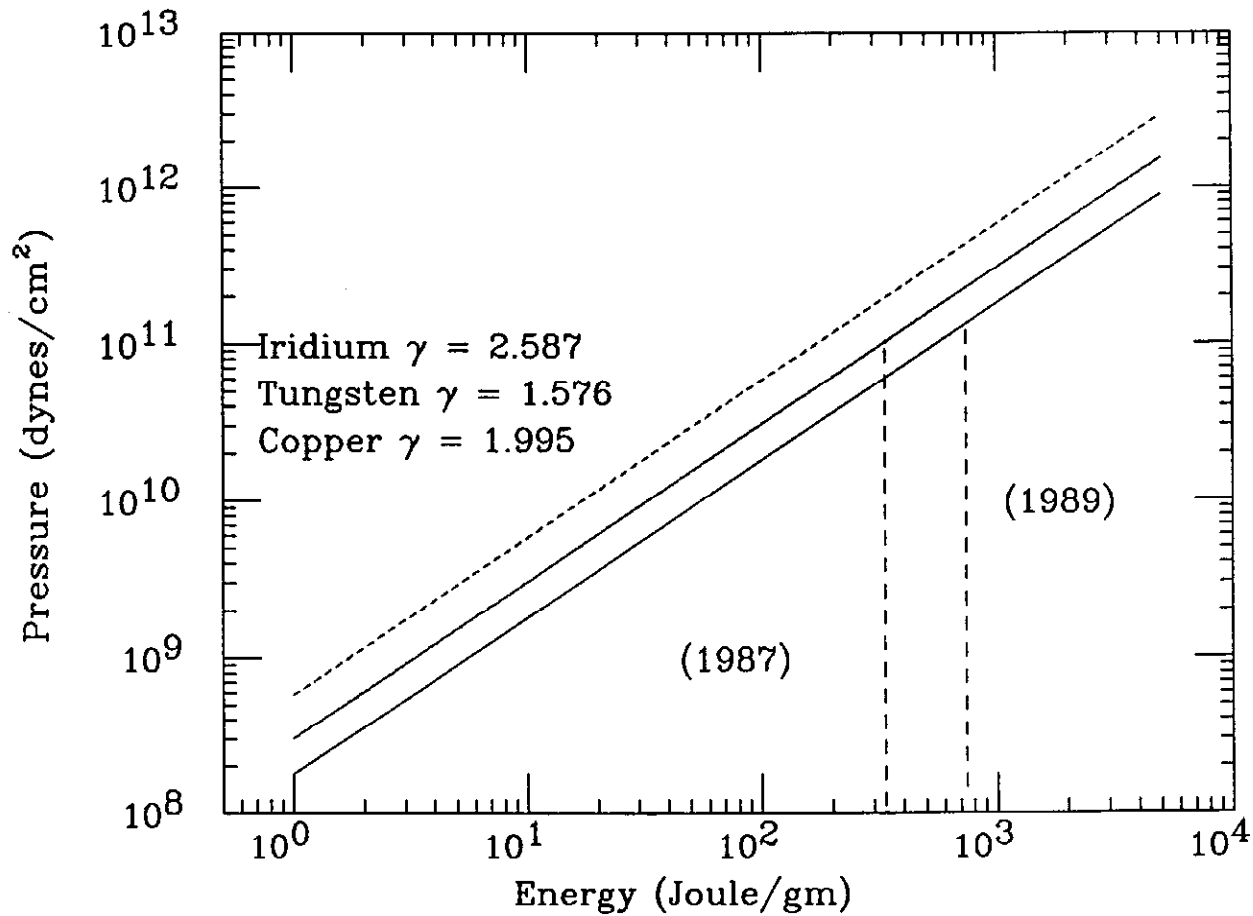
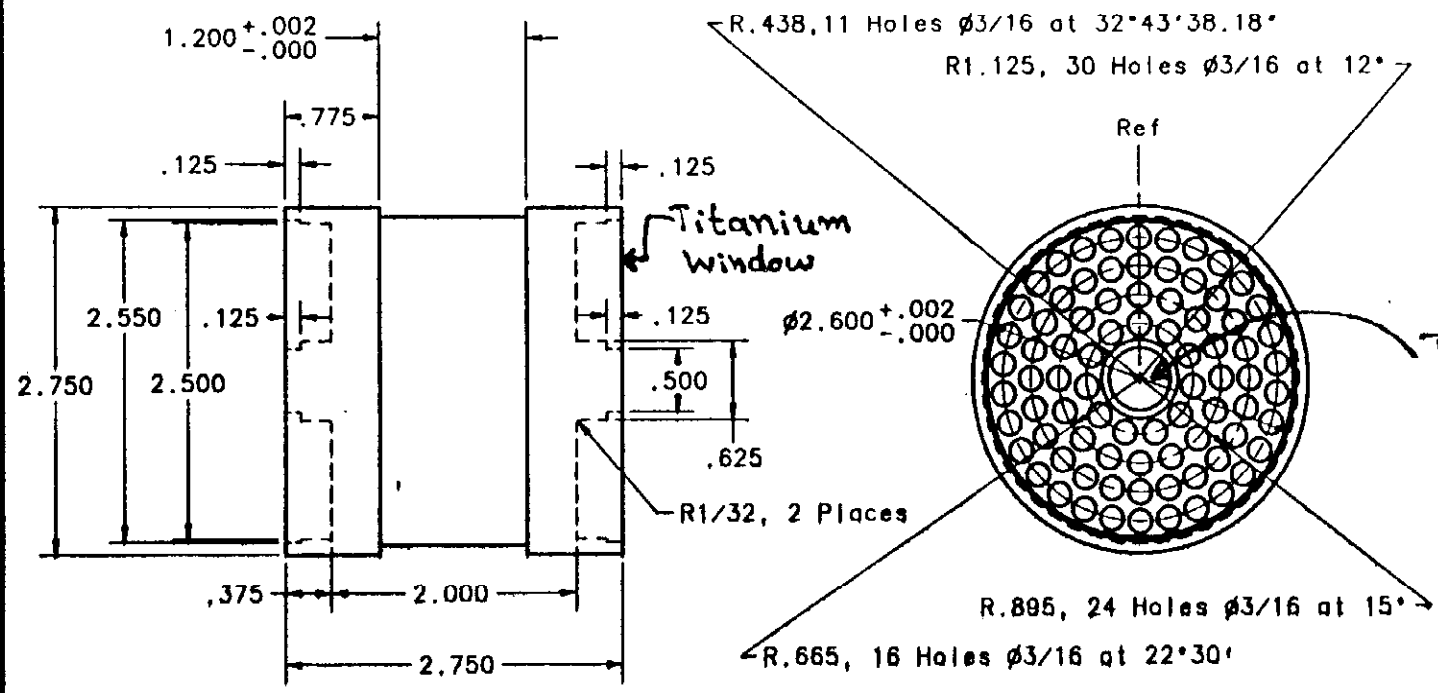


FIG. 4. Pressure vs energy in some of the target materials of interest. γ is the Mie-Gruneisen coefficient. The dashed lines indicate projected pressure developed in the target during 1987 and 1989 collider runs.

A New Target Design for \bar{p} source.

Material: Cu



Target Region

- Efficient Cooling
- Good for Shockwave Absorption

ITEM	PART NO.	DESCRIPTION OR SIZE	QTY.
PARTS LIST			
UNLESS OTHERWISE SPECIFIED	ORIGINATOR	Kr i s Anderson	8/2/90
DECIMALS	FRACTIONS	DRAWN	Kr i s Anderson
2 .005 ± 1/4"		CHECKED	
1. VERIFY ALL DIMENSIONS	APPROVED		
2. DO NOT SCALE DRAWING	USED ON		
3. VERIFY DIMENSIONS			
4. USE ALL DIM. SURFACES	MATERIAL	OFHC Copper	
# FERMIL NATIONAL ACCELERATOR LABORATORY UNITED STATES DEPARTMENT OF ENERGY			
Air Cooled P-bar Target			
REV.	DATE	APPROVED	BY
P1.1			A
CREATED WITH I-DEAS 4.1 USER NAME:			

FIG. 5. A copper target module, newly designed and planned to use during next collider run.

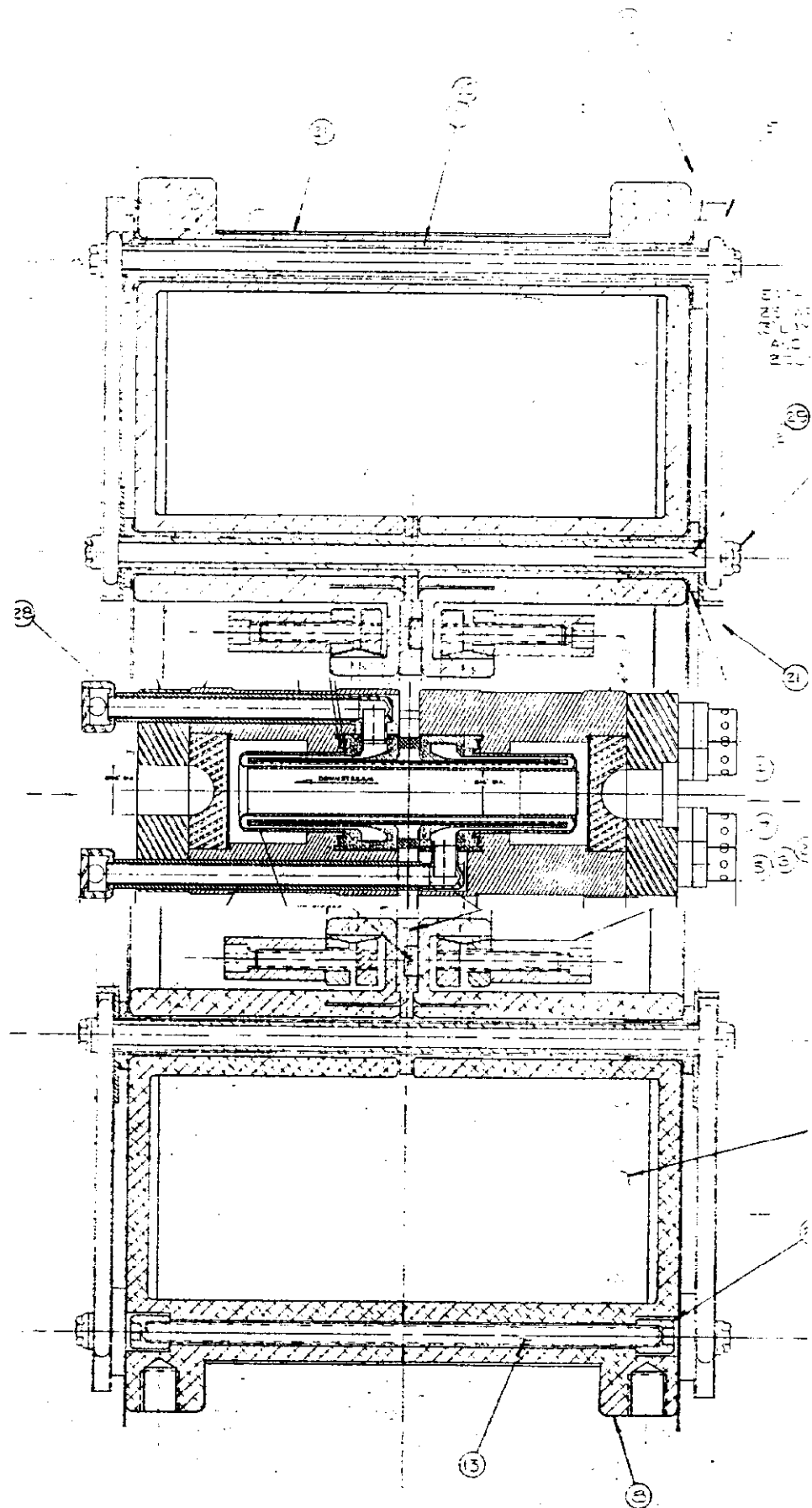


FIG. 6. Li lens being used at Fermilab during 1987 and 1989 collider runs.